2022

Effect of Metal Foam Integration on The Thermal Regulation Performance of Salt Hydrate-Based Heat Sink

Amr Mohamed Kotb

Sophie Wang

Effect of Metal Foam Integration on The Thermal Regulation Performance of Salt Hydrate-Based Heat Sink

Amr Kotb[1], Sophie Wang[1*]

[1] University of Illinois at Urbana-Champaign, Department of Mechanical Science and Engineering, Champaign, Urbana, Illinois 61801, United States

amrmk2@illinois.edu, wangxf@illinois.edu

[*]Corresponding author

ABSTRACT

Phase change materials (PCMs) have recently become more attractive in thermal management and energy storage applications as they possess the merits of high latent heat of fusion and high energy storage density. However, conventional PCMs are well-known for their defects of low thermal conductivity and volume variation during phase transition. In this work, the transient thermal performance of high-temperature sodium acetate trihydrate with aluminum foam heat sink is investigated. A mathematical model is developed and validated with experimental published data. The thermal performance of sodium acetate trihydrate- aluminum composite is compared to the conventional paraffin-copper foam composite under constant wall temperature and constant heat flux boundary conditions. The effect of metal foam integration and foam porosity, on thermal regulation time and maximum surface temperature, were investigated in the study. The results indicate that the inclusion of cellular metal foam with lower porosity offers a reduction in the surface temperature at the expenses of a shorter regulation time reflecting the enhancement of the effective thermal conductivity. Also, the salt hydrate-aluminum composite provides a better thermal management performance in terms of surface temperature and regulation time at this range of melting temperature compared to paraffin-copper composite. This work has the potential for the improvement of the efficiency of high-temperature phase change material-based heat sinks.

1. INTRODUCTION

In the modern-day, electronic devices technologies have evolved into revolutionary breakthroughs with more innovative applications and increased features. With this growing advancement, the rate of internal heat generation in such devices has considerably increased, especially during heavy operation and charging modes. Failure to effectively dissipate this heat will lead to reliability issues and a shortened operational lifetime, limiting such technologies' development (Murshed and Castro, 2017). Encountering such a limitation, thermal management (TM) methods for the latest models of electronic devices have become increasingly essential to stabilize the base temperature at the desired level, knowing that a 1 ºC reduction in the base temperature can reduce the failure rate by 4% which results in an increased lifetime (P, 1996). In such a manner, different TM systems have been developed (Grimes et al., 2010; Mahmoud et al., 2013). However, passive TM by employing phase change materials (PCMs) has become a more attractive technique due to the high energy storage density and high latent heat of fusion of the PCMs. Such properties make a PCM an effective medium for heat transfer as it releases/absorbs energy when transitioning from one state of matter to another. In addition, it offers this competitive cooling performance while being less bulky, expensive and noisy than the conventional active cooling techniques, making it suitable for the cooling of modern mobile devices. However, aside from their unique ability in storing thermal energy, PCMs are well-known for their weak heat transfer performance caused by their low thermal conductivity. At present, efforts have been made to tackle such a challenge using thermal conductivity enhancers (TCEs), including micro/nanoparticles with higher thermal conductivity (Mahdi and Nsofor, 2016) or adding fins (Duan et al., 2020; Peng et al., 2021; Zhang et al., 2021), heat pipes, cellular foams

(Nada and Alshaer, 2019), and other structures. Sahoo et al. (2016) conducted a comprehensive review of these various TCE approaches, and they came to the conclusion that metal foams are the best choice for use as TCE because of their high surface area to volume ratio.

So far, a great deal of experimental and theoretical studies have been carried out to report the thermal regulation performance of metallic foam/PCM heat sinks. Li et al. (2017) experimentally evaluated the thermal behavior of PCM/copper foam composite with foam porosity of 85% and 95%. It was concluded that more than 50% surface temperature reductions are achieved for PCM/foam modules due to the enhancement of effective thermal conductivity compared to pure PCM. Moreover, it was found that lower foam porosity offers lower surface temperature but at the cost of a shorter thermal regulation time. Arshad et al. (2020) investigated the transient performance of CuO coated PCM/metal-foam heat sink of various filling thickness ratios. The experimental results revealed that the filling thickness ratio of 0.5 offers the best thermal performance for passive cooling. Zhu et al. (2018) studied the influence of the filling height ratio of the copper foam on the transient thermal regulation performance of PCM/foam heat sink. The authors used foam structures with a porosity of 96% but two different PPI of 15 and 30. The results showed that 2/3 partial filling was more economical than complete filling in terms of system weight and material with insignificance sacrifice in performance. Mancin et al. (2015) explored the thermal performance of three different paraffinic PCMs of different melting temperatures of 53 ºC, 57 ºC and 59 ºC using copper metal foam of porosity of 95% and PPI of 5, 10 and 40. They reported that incorporating metallic foam with the PCM led to a reduction in surface temperature and improved the heat transfer rate. Wang et al. (2016) investigated the enhancement in heat transfer of a metal foam/paraffin composite TM system. The copper foam of pore size 2-3 mm and 97.3% porosity was used. The results showed that the inclusion of copper foam reduced the heat storage time by 40% and improved the uniformity of melting and internal heat transfer. Li et al. (2019) numerically studied the thermal behavior of microencapsulated PCM (MEPCM) saturated in copper foam. The authors concluded that the surface temperature of the MEPCM/foam composite was merely 50% of the pure MEPCM at the end of the experiment due to the latent heat absorption of MEPCM and thermal conductivity enhancement of the copper foam. The inclusion of the metal matrix also made the internal temperature distribution more uniform and reduced the internal temperature gradient.

From the reported literature above, most of the existing works focused on paraffinic compounds as PCMs to be used with the metallic matrices. Yet, the use of other PCMs types such as salt hydrates is seldom reported due to their potential problems such as subcooling, corrosivity and phase segregation (Yang et al., 2021). However, salt hydrates possess the merits of relatively higher thermal conductivity and high volumetric latent heat compared to paraffinic waxes. While the previously mentioned problems can be avoided by the proper material selection to ensure salt hydrate-foam compatibility and by applying one of the subcooling suppression methods (Beaupere et al., 2018). Mustaffar et al. (2018) was the first study that attempted to create a salt hydrate-metal foam composite. The results revealed that the effective thermal conductivity for the composite was calculated as 10.8 W/m.K, which was higher than many composites previously studied in their literature review. Therefore, the aim of the present work is to further investigate the thermal regulation performance of sodium acetate trihydrate (SAT)/aluminum foam heat sink, and to compare it to the performance of the conventional paraffin-copper heat sink. Moreover, the influence of metal foam porosity on the thermal behavior of both composites is also investigated in the present study.

2. MATHEMATICAL FORMULATION

2.1 Problem Description

The physical model of this work is a 100×100 mm 2D cavity filled with the PCM infiltrated in metallic foam as illustrated in **Figure 1**. All the wall sides of the cavity are assumed to be perfectly insulated except the left wall is set to two different boundary conditions which are constant temperature and constant heat flux of 90℃ and 3 kW/m^2, respectively.

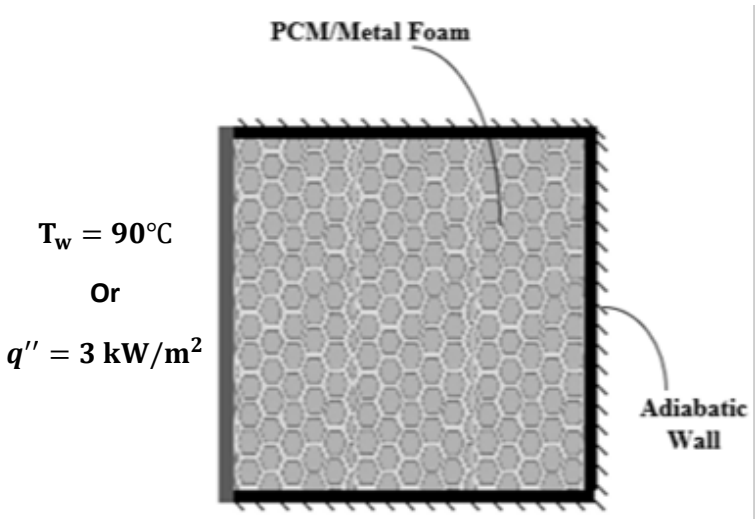

Figure 1: Schematic of PCM/Metal foam model

2.2 Assumptions

The following assumptions are considered in the developed model:

1- PCM liquid phase is incompressible and Newtonian.
2- Laminar flow for the PCM liquid phase.
3- The thermal radiation is neglected in the metal foam.
4- Employing the Boussinesq approximation to account for the density-based buoyancy effect.
5- The metal foam is considered rigid, isotropic and homogeneous.

2.3 Governing Equations

Based on the mentioned assumptions, the equations governing the conservation of mass, momentum, and energy for the present physical model can be concisely formulated as below (Whitaker, 1999) :

Mass Conservation

$$\bar{\nabla}.\bar{V} = 0 \tag{1}$$

Momentum Conservation

$$\frac{\rho_P}{\emptyset}\frac{\partial u}{\partial t} + \frac{\rho_P}{\emptyset^2}\,(\bar{V}\bar{\nabla}).u = -\frac{\partial p}{\partial x} - \left(\frac{\mu}{K} + \frac{\rho_P c_i}{\sqrt{\lambda}}|u|\right)u + \frac{\mu}{\emptyset}\,\nabla^2 u + S_u \tag{2}$$

$$\frac{\rho_P}{\emptyset}\frac{\partial v}{\partial t} + \frac{\rho_P}{\emptyset^2}\,(\bar{V}\bar{\nabla}).v = -\frac{\partial p}{\partial y} - \left(\frac{\mu}{K} + \frac{\rho_P c_i}{\sqrt{\lambda}}|v|\right)v + \frac{\mu}{\emptyset}\,\nabla^2 v + g\beta\rho_P\left(T - T_{ref}\right) + S_v \tag{3}$$

Where K is Permeability and c_i is Inertial Coefficient and they can be calculated using the model of Calmidi, (1998) as expressed in the following equations:

$$K = 0.00073\ d_p^2\ (1-\emptyset)^{-0.224}\left(\frac{d_f}{d_p}\right)^{-1.11} \tag{4}$$

$$c_i = 0.00212\ d_p^2\ (1-\emptyset)^{-0.132}\left(\frac{d_f}{d_p}\right)^{-1.63} \tag{5}$$

$$\frac{d_f}{d_p} = 1.18\sqrt{\frac{1-\emptyset}{\pi}}\left(\frac{1}{1-e^{-(1-\emptyset)/0.04}}\right) \tag{6}$$

$$d_p = \frac{0.0254}{\Upsilon} \tag{7}$$

while S_u, S_v are source terms for velocity damping in solid phase and can be calculated using Carmen-Konzey relation as follows:

$$S_u = \frac{A_m\,(1-\delta)^2}{B^3+\delta}u \tag{8}$$

$$S_v = \frac{A_m(1-\delta)^2}{B^3+\delta}v \tag{9}$$

A_m is the mushy zone constant which is set at $10^5$and B is a small value constant to avoid the division by zero and it is set at 10^{-3}. While $\delta(T)$ can be defined as:

$$\delta(T) = \begin{cases} 0 & T < (T_m - \frac{\Delta T}{2}) \\ \dfrac{T - T_m + \frac{\Delta T}{2}}{\Delta T} & \left(T_m - \frac{\Delta T}{2}\right) \le T < (T_m + \frac{\Delta T}{2}) \\ 1 & T \ge (T_m + \frac{\Delta T}{2}) \end{cases} \tag{10}$$

Energy Conservation

1) PCM

$$\emptyset\rho_P C_{P_P}\frac{\partial T_P}{\partial \mathrm{t}} + \rho_P C_{P_P}\left(u\frac{\partial T_P}{\partial x} + v\frac{\partial T_P}{\partial x}\right) = \lambda_P\nabla^2 T_P + h_{PM}a_{PM}(T_M - T_P) \tag{11}$$

$$\rho_P(T) = \delta\left(\rho_{P_l} - \rho_{P_s}\right) + \rho_{P_s} \tag{12}$$

The interval of phase change temperature in calculations is 3℃ (Aadmi et al., 2014). The PCM heat capacity can be calculated by:

$$C_{P_P} = \delta\left(C_{P_{Pl}} - C_{P_{Ps}}\right) + C_{P_{Ps}} + L_f D(T) \tag{13}$$

$$D(T) = e^{\left(\frac{-(T-T_m)^2}{(\Delta T/4)^2}/\sqrt{\pi(\Delta T/4)^2}\right)} \tag{14}$$

Where L_f is the specific latent heat of fusion of the PCM and D is Delta Dirac function which has a unity integral to ensure the conservation of latent heat during melting. The PCM thermal conductivity can be expressed as:

$$\lambda_{Pe}(T) = \delta(\lambda_{Pl} - \lambda_{Ps}) + \lambda_{Ps} \tag{15}$$

2) Metallic foam

$$(1-\emptyset)\rho_M C_{P_M}\frac{\partial T_M}{\partial t} = \lambda_{Me}\nabla^2 T_M - h_{PM}a_{PM}(T_M - T_P) \tag{16}$$

Where λ_{P_e} and λ_{M_e} are the effective thermal conductivity of PCM and metal foam, respectively. a_{PM} is the specific area and can be calculated using:

$$a_{PM} = \frac{3\pi d_f\left(1 - e^{-((1-\emptyset)/0.004)}\right)}{\left(0.59 d_p\right)^2} \tag{17}$$

While h_{PM} is the interstitial heat transfer coefficient between the PCM and the metal foam and can be estimated as (Lu et al., 2006):

$$h_{PM} = \begin{cases} 0.76\mathrm{Re}^{0.4}\ \mathrm{Pr}^{0.37}\ \dfrac{\lambda_P}{d} & 0 < \mathrm{Re} \leq 40 \\ 0.52\mathrm{Re}^{0.5}\ \mathrm{Pr}^{0.37}\ \dfrac{\lambda_P}{d} & 40 < \mathrm{Re} \leq 1000 \\ 0.26\mathrm{Re}^{0.6}\ \mathrm{Pr}^{0.37}\ \dfrac{\lambda_P}{d} & 1000 < \mathrm{Re} \leq 20000 \end{cases} \tag{18}$$

While the corrected model of Boomsma and Poulikakos model (Dai et al., 2010) was used in describing the effective thermal conductivity as expressed in equations (19-27):

$$\lambda_{Pe} = \lambda_{eff} \mid \lambda_s = 0 \tag{19}$$

$$\lambda_{Me} = \lambda_{eff} \mid \lambda_l = 0 \tag{20}$$

$$\lambda_{eff} = \frac{\sqrt{2}}{2(R_A + R_B + R_C + R_D)} \tag{21}$$

$$R_A = \frac{4d}{(2e^2 + \pi d(1-e))\lambda_s + (4 - 2e^2 - \pi d(1-e))\lambda_l} \tag{22}$$

$$R_B = \frac{(e - 2d)}{e^2\lambda_s + (2 - e^2)\lambda_l} \tag{23}$$

$$R_C = \frac{(\sqrt{2} - 2e)}{\pi d^2\sqrt{2}\lambda_s + \left(2 - \pi d^2\sqrt{2}\right)\lambda_l} \tag{24}$$

$$R_D = \frac{2e}{e^2\lambda_s + (4 - e^2)\lambda_l} \tag{25}$$

$$d = \sqrt{\frac{\sqrt{2}\left(2 - (3/4)e^3\sqrt{2} - 2\emptyset\right)}{\pi(3 - 4e\sqrt{2} - e)}} \tag{26}$$

$$e = 0.339 \tag{27}$$

2.4 Numerical Procedure

The proposed model is solved using finite element method with COMSOL Multiphysics ®. The heat and fluid flow has been modeled and solved using Heat Transfer in Fluids and Brinkman Equation models, respectively. Heat Transfer in Solids model is used to model the porous matrix. Local non-thermal equilibrium interface is used to couple the heat transfer in the PCM and the metal foam. The 2D problem under consideration has been meshed into 29,072 triangular elements to form an entirely structured grid everywhere in the domain. Additionally, the independence test of time step was performed. The optimal value was considered as 1 s.

2.5 Model Validation

To assess the accuracy of the numerical results, the present model was validated by feeding the model with the data from (Zhang et al., 2017) and compare their experimental data of average temperatures of PCM and foam ligaments to the results from the present model. The literature setup consists of 100mm×100mm×10mm unit of paraffin-copper foam composite with 97% and 25PPI porosity and foam density, respectively. As shown in **Figure 2**, the trend of changes in both experimental and numerical results is the same and shows good agreement in values with a maximum deviation of 6.8%. This indicates the accuracy and applicability of the present model.

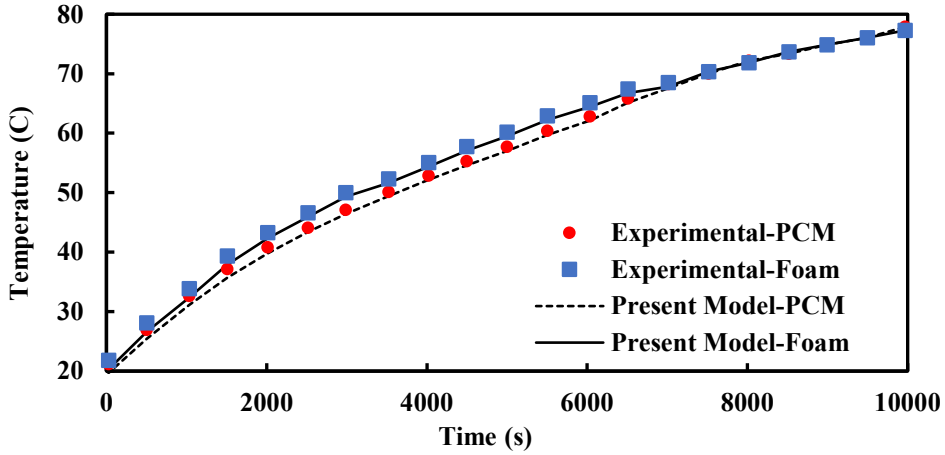

Figure 2: Comparison of present model with the experimental data in literature (Zhang et al., 2017)

3. RESULTS AND DISCUSSION

In this section, we compare the thermal regulation performance of two different PCM/Foam composites with comparable melting temperatures which are RT60/copper foam and Sodium Acetate Trihydrate (SAT)/aluminum foam. The reason behind choosing aluminum for the SAT is its high corrosion resistance against SAT compared to copper (Medrano et al., 2009) . In addition, the effect of foam porosity on the thermal performance is investigated under two different left wall boundary conditions. The thermophysical properties of all materials under investigation were listed in **Table 1**.

Table 1: Thermophysical properties of PCM and metal foam

	PCM			**Metal Foam**	
	RT60	**SAT**		**Copper**	**Aluminum**
Melting range (℃)	56-62	57-62	**Density (kg/m^3)**	8933	2800
Density (kg/m^3) (Solid/Liquid)	880/770	1450/1280	**Heat capacity (J/kg.K)**	380	910
Heat capacity (J/kg.K) (Solid/Liquid)	1800/2000	1970/3350	**Thermal conductivity (W/m.K)**	400	237
Thermal conductivity (W/m.K) (Solid/Liquid)	0.24/0.2	0.7/0.7	**Foam density**	10 PPI	10 PPI
Latent heat (kJ/kg)	160	264			
Dynamic viscosity (Pa.s)	2.508×10^{-3}	1.122×10^{-3}			

3.1 Constant wall temperature

The effect of foam porosity on the liquid fraction evolution and complete melting time is investigated for the two PCM-foam composites. The left wall temperature is fixed at 90℃ while the initial temperature of the whole system is set at 40℃. **Figure 3** illustrates the change of average liquid fraction with time for foam porosities of 85%, 90%, 95% and 100% (Pure PCM) for both RT60-copper and SAT-aluminum composites. It can be seen that the rising speed of the average liquid fraction was reduced considerably with the metal foam integration. In addition, the melting rate is further increased with the porosity reduction. This indicates the enhancement in heat transfer and thermal penetration associated with porosity reduction. The reason behind this is that the lower the foam porosity, the larger the metal foam volume fraction and hence the higher the effective thermal conductivity enhancement. Moreover, a slower liquid fraction evolution is observed in case of SAT-aluminum due to the higher density and higher volumetric latent heat of SAT, and the relatively lower effective thermal conductivity of SAT-aluminum compared to RT60-copper. For such reasons, the complete melting time of SAT-aluminum composite is generally higher than the other composite as shown in **Figure 4**. For example, the melting time of pure SAT is 227s longer than the RT60-copper case. It can also be observed that the melting time decreases with the porosity increase for both composites. However, the reduction in melting time become more insignificant as the porosity decreases. For instance, reducing the aluminum foam porosity from 95% to 90% saves 184s in melting time, while the time saved from 90% to 85% foam porosity is merely 63s.

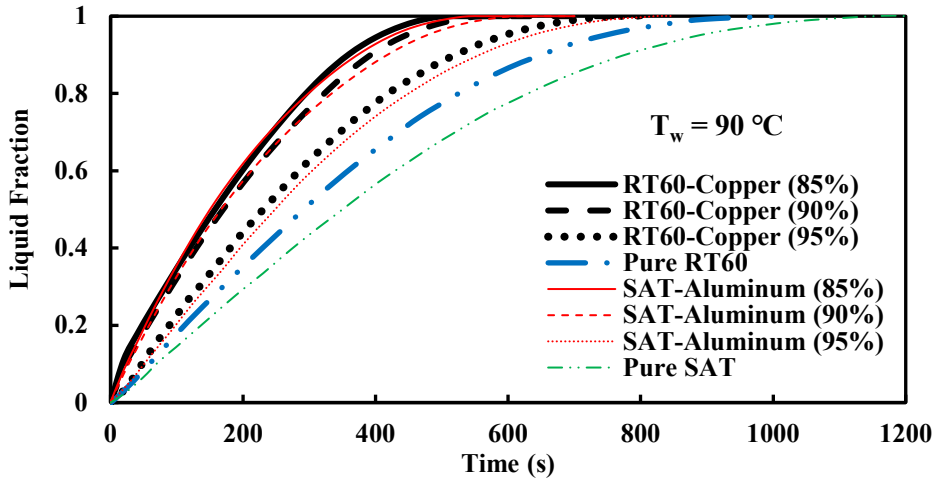

Figure 4: Liquid fraction variation with time at different foam porosities and different PCM-foam composites (T_w=90℃)

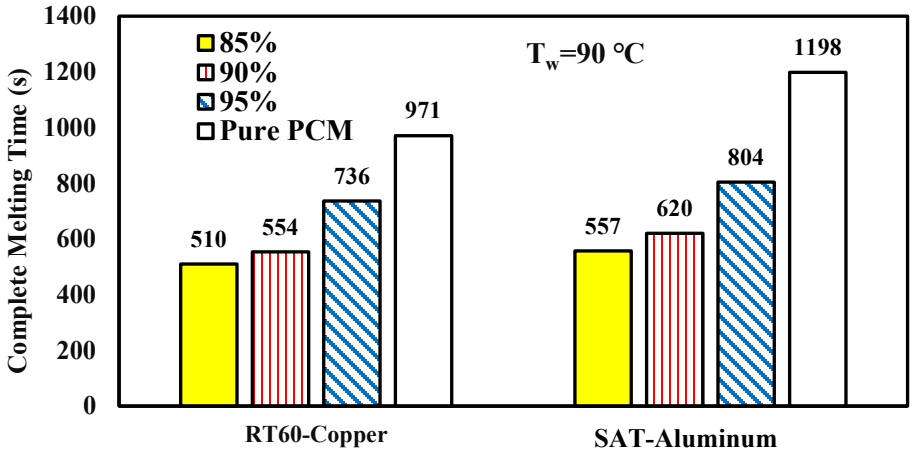

Figure 3: Complete melting time for different porosities and different PCM-foam composites (T_w= 90℃)

3.2 Constant heat flux

In this section, the thermal regulation performance of both PCM-foam composites is investigated in terms of left wall temperature and the thermal regulation time. To mimic the thermal management of electronic devices that generate a constant heat flux, the left wall temperature is subjected to heat flux of $3\ \mathrm{kW/m^2}$ while the initial temperature of the whole system is set at 40℃. **Figure 5** shows the history of left wall temperature response for RT60-copper and SAT-aluminum composites with foam porosities of 85%, 90% and 95%. Generally, it is clear that lower foam porosities obtain lower average wall temperature during phase change due to the higher effective thermal conductivity and larger interfacial area. However, such reduction in the wall temperature at lower foam porosity is achieved at the cost of shortening the thermal regulation time. For example, reducing the copper foam porosity from 95% to 85% leads to 4℃ decrease in the wall temperature during phase change and a reduction of 16.7% in the thermal management time just before the sharp increase in wall temperature after complete melting. Additionally, SAT-aluminum composite offers much longer regulation time and lower wall temperature at all porosities compared to paraffin case. After 6000s of heating cycle, the SAT-aluminum average wall temperature is lower by 35% than its value for RT60-copper case. This indicates the better thermal management performance of SAT-aluminum composite at this range of melting temperature.

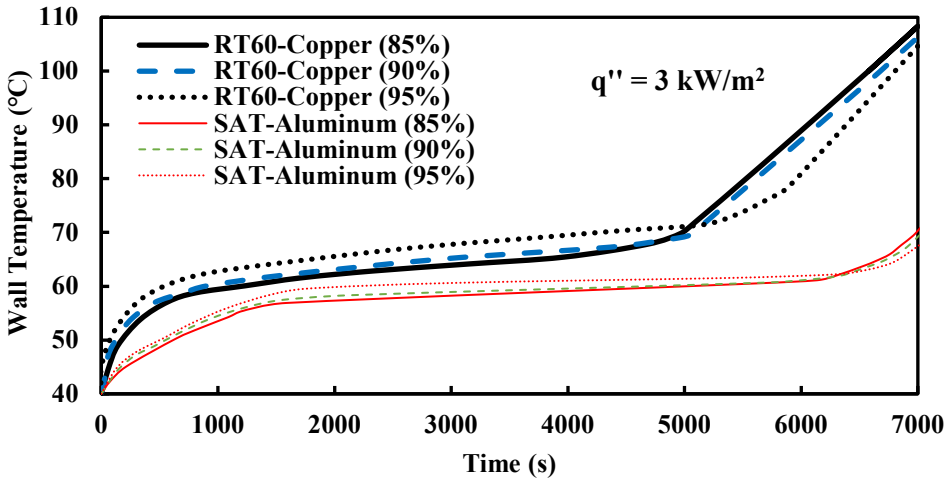

Figure 5: Variation of left wall temperature with time at different porosities and different PCM-foam composites (q" = 3 kW/m^2)

4. CONCLUSION

This paper addresses the thermal regulation performance of salt hydrate-based high temperature heat sink A thorough mathematical model for a square PCM based heat sink is built and solved numerically using COMSOL Multiphysics ®. A comparison of the thermal performance between sodium acetate trihydrate-aluminum and paraffin-copper composites is conducted. The effect of metallic matrix integration and matrix porosity on the thermal regulation time, melting rate and surface temperature have been reported. The following conclusions can be extracted:

- For constant wall temperature of 90℃, the pure SAT takes 227 sec longer time for complete melting compared to RT60-copper due to the higher thermal volumetric latent heat and higher density. Additionally, integrating aluminum foam with porosities of 85% and 90% to the SAT reduces the complete melting time by 53.5% and 48.2%, respectively.

- For constant heat flux of $3\ \mathrm{kW/m^2}$ subject to the wall, increasing the foam porosity leads to an increase in thermal regulation time at the cost of higher surface temperature. The SAT-aluminum composite offered a

longer thermal regulation time compared to RT60-copper composite. In addition, the SAT-aluminum average surface temperature is lower by 35% than its value for RT60-copper case.

NOMENCLATURE

A_m	Mushy zone constant	(-)
a_{PM}	Specific area	(m^2)
c_i	Inertial coefficient	(W/m^2K)
C_p	Specific heat capacity	(J/kg.K)
d	Diameter	(m)
g	Gravitational acceleration	(m/s^2)
h_{PM}	Interstitial heat transfer coefficient	(W/m^2K)
K	Permeability	(m^2)
L_f	Specific latent heat of fusion	(J/kg)
p	Pressure	(N/m^2)
q''	Heat flux	(kW/m^2)
R	Simplification quantity	(m.K/W)
t	Time	(s)
T	Temperature	(K)
T_m	Melting temperature	
u, v	Local velocities	(K)
$\bar{V}$	Velocity vector	(m/s)
x, y	Cartesian coordinates directions	(m/s)
		(-)

Greek Symbols

ρ	Density	(kg/m^3)
$\emptyset$	Porosity	(-)
μ	Dynamic Viscosity	($N.s/m^2$)
β	Thermal Expansion Coefficient	(1/K)
λ	Thermal Conductivity	(W/m K)
Υ	Foam Density	(PPI)

Subscripts

A,B,C,D	Unit cell subsections
e	Equivalent
eff	Effective
f	Fiber
l	Liquid
M	Metal foam
p	Pore
P	PCM
ref	Reference
s	Solid
w	Wall

REFERENCES

Aadmi, M., Karkri, M., & el Hammouti, M. (2014). Heat transfer characteristics of thermal energy storage of a composite phase change materials: Numerical and experimental investigations. *Energy*, *72*, 381–392.

Arshad, A., Jabbal, M., & Yan, Y. (2020). Thermal Performance of PCM-based Heat Sink with Partially Filled Copper Oxide Coated Metal-foam for Thermal Management of Microelectronics. *2020 19th IEEE Intersociety Conference on Thermal and Thermomechanical Phenomena in Electronic Systems (ITherm)*, 697–702.

Beaupere, N., Soupremanien, U., & Zalewski, L. (2018). Nucleation triggering methods in supercooled phase change materials (PCM), a review. In *Thermochimica Acta* (Vol. 670, pp. 184–201). Elsevier B.V.

Calmidi, V. v. (1998). *Transport phenomena in high porosity fibrous metal foams*. University of Colorado.

Dai, Z., Nawaz, K., Park, Y. G., Bock, J., & Jacobi, A. M. (2010). Correcting and extending the Boomsma-Poulikakos effective thermal conductivity model for three-dimensional, fluid-saturated metal foams. *International Communications in Heat and Mass Transfer*, *37*(6), 575–580.

Duan, J., Xiong, Y., & Yang, D. (2020). Study on the effect of multiple spiral fins for improved phase change process. *Applied Thermal Engineering*, *169*.

Grimes, R., Walsh, E., & Walsh, P. (2010). Active cooling of a mobile phone handset. *Applied Thermal Engineering*, *30*(16), 2363–2369.

Li, W., Hou, R., Wan, H., Liu, P., He, G., & Qin, F. (2017). A new strategy for enhanced latent heat energy storage with microencapsulated phase change material saturated in metal foam. *Solar Energy Materials and Solar Cells*, *171*, 197–204.

Li, W. Q., Wan, H., Jing, T. T., Li, Y. B., Liu, P. J., He, G. Q., & Qin, F. (2019). Microencapsulated phase change material (MEPCM) saturated in metal foam as an efficient hybrid PCM for passive thermal management: A numerical and experimental study. *Applied Thermal Engineering*, *146*, 413–421.

Lu, W., Zhao, C. Y., & Tassou, S. A. (2006). Thermal analysis on metal-foam filled heat exchangers. Part I: Metal-foam filled pipes. *International Journal of Heat and Mass Transfer*, *49*(15–16), 2751–2761.

Mahdi, J. M., & Nsofor, E. C. (2016). Solidification of a PCM with nanoparticles in triplex-tube thermal energy storage system. *Applied Thermal Engineering*, *108*, 596–604.

Mahmoud, S., Tang, A., Toh, C., AL-Dadah, R., & Soo, S. L. (2013). Experimental investigation of inserts configurations and PCM type on the thermal performance of PCM based heat sinks. *Applied Energy*, *112*, 1349–1356.

Mancin, S., Diani, A., Doretti, L., Hooman, K., & Rossetto, L. (2015). Experimental analysis of phase change phenomenon of paraffin waxes embedded in copper foams. *International Journal of Thermal Sciences*, *90*, 79–89.

Medrano, M., Yilmaz, M. O., Nogués, M., Martorell, I., Roca, J., & Cabeza, L. F. (2009). Experimental evaluation of commercial heat exchangers for use as PCM thermal storage systems. *Applied Energy*, *86*(10), 2047–2055.

Mustaffar, A., Reay, D., & Harvey, A. (2018). The melting of salt hydrate phase change material in an irregular metal foam for the application of traction transient cooling. *Thermal Science and Engineering Progress*, *5*, 454–465.

Nada, S. A., & Alshaer, W. G. (2019). Experimental investigation of thermal conductivity enhancement of carbon foam saturated with PCM and PCM/MWCNTs composite for energy storage systems. *Heat and Mass Transfer/Waerme- Und Stoffuebertragung*.

P, M. (1996). Design of experiment based evaluation of the thermal performance of a flipchip electronic assembly. *ASME. EEP (American Society of Mechanical Engineers. Electrical and Electronic Packaging Div.)*, *18*, 109–115.

Peng, B., He, Z., Wang, H., & Su, F. (2021). Optimization of patterned-fins for enhancing charging performances of phase change materials-based thermal energy storage systems. *International Journal of Heat and Mass Transfer*, *164*.

Sahoo, S. K., Das, M. K., & Rath, P. (2016). Application of TCE-PCM based heat sinks for cooling of electronic components: A review. In *Renewable and Sustainable Energy Reviews* (Vol. 59, pp. 550–582). Elsevier Ltd.

Sohel Murshed, S. M., & Nieto de Castro, C. A. (2017). A critical review of traditional and emerging techniques and fluids for electronics cooling. *Renewable and Sustainable Energy Reviews*, *78*, 821–833.

Wang, C., Lin, T., Li, N., & Zheng, H. (2016). Heat transfer enhancement of phase change composite material: Copper foam/paraffin. *Renewable Energy*, *96*, 960–965.

Whitaker. (1999). The Method of Volume Averaging. In *Theory and Applications of Transport in Porous Media* (Vol. 13). Springer Netherlands.

Yang, T., King, W. P., & Miljkovic, N. (2021). Phase change material-based thermal energy storage. In *Cell Reports Physical Science* (Vol. 2, Issue 8). Cell Press.

Zhang, D., Zhang, F., Tang, S., Guo, C., & Qin, X. (2021). Performance evaluation of cascaded storage system with multiple phase change materials. *Applied Thermal Engineering*, *185*.

Zhang, P., Meng, Z. N., Zhu, H., Wang, Y. L., & Peng, S. P. (2017). Melting heat transfer characteristics of a composite phase change material fabricated by paraffin and metal foam. *Applied Energy*, *185*, 1971–1983.

Zhu, Z. Q., Huang, Y. K., Hu, N., Zeng, Y., & Fan, L. W. (2018). Transient performance of a PCM-based heat sink with a partially filled metal foam: Effects of the filling height ratio. *Applied Thermal Engineering*, *128*, 966–972.